ORIGINAL ARTICLE

JBMR®

Female Mice Lacking Estrogen Receptor-Alpha in Osteoblasts Have Compromised Bone Mass and Strength

Katherine M Melville,[1,2] Natalie H Kelly,[1,2] Sohaib A Khan,[3] John C Schimenti,[4] F Patrick Ross,[5] Russell P Main,[6,7] and Marjolein C H van der Meulen[1,5]

[1]Sibley School of Mechanical and Aerospace Engineering, Cornell University, Ithaca, NY, USA
[2]Department of Biomedical Engineering, Cornell University, Ithaca, NY, USA
[3]College of Medicine, University of Cincinnati, Cincinnati, OH, USA
[4]College of Veterinary Medicine, Cornell University, Ithaca, NY, USA
[5]Research Division, Hospital for Special Surgery, New York, NY, USA
[6]College of Veterinary Medicine, Purdue University, West Lafayette, IN, USA
[7]Weldon School of Biomedical Engineering, Purdue University, West Lafayette, IN, USA

ABSTRACT

Reduced bioavailability of estrogen increases skeletal fracture risk in postmenopausal women, but the mechanisms by which estrogen regulates bone mass are incompletely understood. Because estrogen signaling in bone acts, in part, through estrogen receptor alpha (ERα), mice with global deletion of ERα (ERαKO) have been used to determine the role of estrogen signaling in bone biology. These animals, however, have confounding systemic effects arising from other organs, such as increased estrogen and decreased insulin-like growth factor 1 (IGF-1) serum levels, which may independently affect bone. Mice with tissue-specific ERα deletion in chondrocytes, osteoblasts, osteocytes, or osteoclasts lack the systemic effects seen in the global knockout, but show that presence of the receptor is important for the function of each cell type. Although bone mass is reduced when ERα is deleted from osteoblasts, no study has determined if this approach reduces whole bone strength. To address this issue, we generated female osteoblast-specific ERαKO mice (pOC-ERαKO) by crossing mice expressing a floxed ERα gene ($ER\alpha^{fl/fl}$) with mice transgenic for the *osteocalcin-Cre* promoter (*OC-Cre*). Having confirmed that serum levels of estrogen and IGF-1 were unaltered, we focused on relating bone mechanics to skeletal phenotype using whole bone mechanical testing, microcomputed tomography, histology, and dynamic histomorphometry. At 12 and 18 weeks of age, pOC-ERαKO mice had decreased cancellous bone mass in the proximal tibia, vertebra, and distal femur, and decreased cortical bone mass in the tibial midshaft, distal femoral cortex, and L5 vertebral cortex. Osteoblast activity was reduced in cancellous bone of the proximal tibia, but osteoclast number was unaffected. Both femora and vertebrae had decreased whole bone strength in mechanical tests to failure, indicating that ERα in osteoblasts is required for appropriate bone mass and strength accrual in female mice. This pOC-ERαKO mouse is an important animal model that could enhance our understanding of estrogen signaling in bone cells in vivo. © 2014 American Society for Bone and Mineral Research.

KEY WORDS: GENETIC ANIMAL MODELS; SEX STEROIDS; OSTEOBLASTS; OSTEOPOROSIS; BIOMECHANICS

Introduction

Osteoporosis, characterized by low bone mass, greatly increases skeletal fracture risk. Each year in the United States, osteoporotic fractures affect 1.5 million individuals and cost $17 billion in treatment.[1] As a result of the increasingly aged population, by 2025 treatment costs are predicted to rise to $25 billion.[2] To reduce this economic burden and the cost of patient suffering, clinical strategies to maintain and even increase bone mass are essential and require understanding the complexity of cell signaling in bone.

Bone mass is regulated by a number of factors, including the sex hormones estrogen and testosterone, circulating parathyroid hormone (PTH) and insulin-like growth factor 1 (IGF-1), and biophysical stimuli including the mechanical environment. By suppressing bone resorption and remodeling, estrogen regulates bone mass in both men and women during pubertal growth and throughout adulthood.[3–5] At the onset of menopause, women experience a sharp decline in circulating estrogen that is accompanied by decreased bone mineral density, which can lead to osteoporosis and increased fracture risk.[6,7] Primarily due to this rapid hormonal decline, the majority of osteoporosis-

Received in original form April 2, 2013; revised form August 2, 2013; accepted August 17, 2013. Accepted manuscript online August 27, 2013.
Address correspondence to: Marjolein C H van der Meulen, PhD, Sibley School of Mechanical and Aerospace Engineering, Cornell University, 219 Upson Hall, Ithaca, NY 14853, USA. E-mail: mcv3@cornell.edu
Additional Supporting Information may be found in the online version of this article.
Journal of Bone and Mineral Research, Vol. 29, No. 2, February 2014, pp 370–379
DOI: 10.1002/jbmr.2082

related fractures occur in women.[8] However, reduced bone mass and unfused growth plates were found in a male with an inactivating point mutation in the estrogen receptor alpha (ERα) gene, indicating that estrogen plays a role in bone mass in both sexes.[9] Other research has also highlighted the importance of estrogen in the male skeleton and the pathogenesis of osteoporosis.[10]

Although estrogen acts through two ERs, ERα and ERβ, coded by separate genes, the steroid impacts bone mainly via ERα, which is present in chondrocytes, osteoblasts, osteocytes, and osteoclasts.[3] Studies of global ERα knockout (ERαKO) mice show that ERα has a profound effect on bone tissue in growing and adult animals.[11–13] Focusing on females, ERαKO mice had shorter bones compared to littermate controls during growth and maturation, in addition to increased cancellous and cortical bone mineral density in the tibia.[14–17] Importantly, estrogen acts through ERα and/or ERβ in many organ systems, not limited to bone, resulting in confounding systemic effects in female global ERαKO mice, including increased body and uterine masses.[15,17] Also, serum levels of estrogen and testosterone were both increased,[12,17,18] whereas that of serum IGF-1 was decreased.[17] Because estrogen and IGF-1 are major independent regulators of bone mass, the role of ERα in bone is difficult to isolate and interpret in mice lacking the gene globally. Given these facts, a logical approach is to delete the gene in individual bone cell types with the goal of gaining a better understanding of the cell-specific effects of estrogen signaling, knowledge that will contribute to prevention of fractures and new treatments for osteoporosis.

Recent generation of bone-specific ERαKO mice revealed that expression of the receptor in chondrocytes, osteoblast progenitors, osteoblasts, osteocytes, or osteoclasts is important for maintaining bone mass during both growth and aging. However, the relationships between ERα and cancellous and cortical bone in females and males are complex and conflicting.[19–23] Osteoclast-specific female ERαKO mice exhibited osteoporosis with cancellous architecture similar to that seen in postmenopausal women, as a result of reduced apoptosis of osteoclasts and subsequent high bone turnover rates, but cortical bone was unaffected.[22,23] When ERα was deleted from osteoblast progenitors, cortical but not cancellous bone mass was reduced in males and females.[19] In osteocyte-specific ERαKO mice, cortical bone was unaffected in both sexes, whereas cancellous bone was reduced in males but not females.[21] Use of *OC-Cre* mice to delete ERα in osteoblasts reduced cancellous and cortical bone mass in females only, but no changes in bone mass in either sex were found when the gene was deleted in osteoblasts using *col1a1-Cre* mice.[19,20] To study the skeletal structural compromise that occurs with osteoporosis, bone strength, which is dependent upon bone mass, bone architecture, and material properties, must be considered.[24] Importantly, the effect of ERα deletion in osteoblasts on whole bone strength at cortical and cancellous sites has not been studied in these models.

Therefore, the aim of this work was to determine the role of ERα in osteoblasts and osteocytes on cortical and cancellous bone mass and strength. To this end, we bred female osteoblast-specific ERαKO mice using the *osteocalcin-Cre* mouse. Having eliminated the possible role of systemic effects, we focused on relating bone mechanics to skeletal phenotype using microcomputed tomography (μCT), histology, dynamic histomorphometry, and whole-bone mechanical testing in growing and skeletally mature mice.

Subjects and Methods

Generation of osteoblast-specific ERαKO mice (pOC-ERαKO)

pOC-ERαKO mice were generated by breeding mice with exon 3 of the DNA-binding domain of the ERα gene (*Esr1*) flanked by loxP sequences, $ERα^{fl/fl}$,[13] to mice containing a transgene encoding *Cre* recombinase driven by the human osteocalcin promoter, *OC-Cre*, provided by Dr. Thomas Clemens (The Johns Hopkins University, Baltimore, MD, USA).[25,26] The resulting compound heterozygous mice, $OC\text{-}Cre;ERα^{fl/+}$, were bred back to $ERα^{fl/fl}$ mice to produce female osteoblast-specific ERα knockout mice, $OC\text{-}Cre;ERα^{fl/fl}$ (pOC-ERαKO), and littermate controls, $ERα^{fl/+}$ (LC). The *OC-Cre* mice were inbred to the C57Bl/6 strain, whereas $ERα^{fl/fl}$ mice were on a mixed C57Bl/6 and 129Sv background. Mice were housed 3 to 5 per cage with 12-hour:12-hour light:dark cycles with *ad libitum* access to food and water. All animal procedures were approved by Cornell University's Institutional Animal Care and Use Committee.

Mouse genotyping was conducted by lysed tail PCR using the primers: 5′-CAAATAGCCCTGGCAGAT-3′ (forward) and 5′-TGATACAAGGGACATCTTCC-3′ (reverse) to detect the *Cre* transgene, whereas the floxed ERα gene was detected using the primers: 5′-TGGGTTGCCCGATAACAATAAC-3′ (forward) and 5′-AAGAGATGTAGGGCGGGAAAAG-3′ (reverse).

Femoral shaft DNA was purified for PCR to detect the floxed ERα gene using the primers above. Briefly, femora were dissected, the bone marrow was flushed, and bone ends were cut off to isolate the diaphysis. DNA purification was performed following the manufacturer's instructions (QIAamp DNA mini kit; Qiagen, Valencia, CA, USA).

Mass and serum hormone measurements

Female LC and pOC-ERαKO mice were aged to 12 weeks (LC, $n = 16$; pOC-ERαKO, $n = 17$) and 18 weeks of age (LC, $n = 10$; pOC-ERαKO, $n = 10$). Body mass was recorded at 4, 8, 12, and 18 weeks of age. Ovarian and uterine mass were measured at 12 and 18 weeks of age. Blood was collected through cardiac puncture at euthanasia, kept on ice for 4 hours, and then stored at 4°C overnight. Blood was centrifuged at $2000 \times g$ for 20 minutes to obtain serum, which was stored at −20°C. Serum was assayed using kits for estrogen (E2; CalBiotech, Spring Valley, CA, USA; EW180S-100), testosterone (T, CalBiotech; 12 week mice only, TE187S-100), osteocalcin (OC; ALPCO, Salem, NH, USA; 31-50-1300), IGF-1 (ALPCO; 22-IGF-R21), and tartrate-resistant acid phosphatase 5b (TRACP5b; IDS, Scottsdale, AZ, USA; SB-TR103). TRACP5b, OC, and IGF-1 assays were performed by the MECORE Laboratory (St. Joseph Hospital, Bangor, ME, USA).

Microcomputed Tomography

Right tibiae were harvested and fixed in 4% paraformaldehyde for 24 hours at 4°C and then transferred to 70% ethanol. Right femora and L5 vertebrae were harvested, wrapped in PBS-soaked gauze, and stored at −20°C. Bones were scanned using μCT at room temperature with an isotropic voxel resolution of 15 μm (μCT35; Scanco Medical AG, Switzerland; 55 kVp, 145 μA, 600 ms integration time). In each tibia, two volumes of interest (VOIs) were analyzed: a cancellous region manually contoured in the proximal tibia excluding the cortical shell beginning ~0.5 mm distal to the growth plate and extending 10% of total bone length, and a cortical region centered at the midshaft and

extending 2.5% of total bone length. In the distal femur, cortical bone was manually separated from cancellous bone beginning ~0.5 mm proximal to the distal growth plate and extending 2 mm proximally. In each vertebra, cortical bone was manually separated from cancellous bone extending the entire height of the vertebra. Measurable outcomes for cancellous regions included bone volume fraction (BV/TV), trabecular thickness (Tb.Th), trabecular separation (Tb.Sp), and cancellous tissue mineral density (cn.TMD). Measurable outcomes for the cortical regions included cortical area (Ct.Ar), marrow area (Ma.Ar, tibia only), total area (T.Ar, tibia only), maximum and minimum moments of inertia (I_{MAX}, I_{MIN}, respectively), cortical thickness (Ct.Th), and cortical tissue mineral density (ct.TMD). Mineralized tissue was separated from nonmineralized tissue using age-specific and bone-specific thresholds.

Dynamic histomorphometry

Ten and 3 days before euthanasia, mice were administered calcein through intraperitoneal injection (30 mg/kg). Left tibiae were dissected at euthanasia and fixed in 70% ethanol. Bones were embedded in acrylosin and sectioned with a D profile tungsten-carbide blade to 5 μm thickness using a rotary microtome (Leica RM2265; Germany) by the Bone Histology/Histomorphometry Laboratory (Yale University Department of Orthopaedics and Rehabilitation, New Haven, CT, USA). Two slides per mouse and 4 to 5 mice per genotype were analyzed to measure single and double fluorescent labels on cancellous bone in longitudinal sections of the proximal tibia and on cortical bone in transverse sections of the tibial midshaft (OsteomeasureXP v3.2.1.7, Osteometrics, Decatur, GA, USA). Outcome measures were mineralizing surface (MS), mineral apposition rate (MAR), and bone formation rate (BFR).

Histology

After μCT scanning, right tibiae from both 12-week-old and 18-week-old animals were decalcified for 2 weeks in 10% EDTA, embedded in paraffin, and sectioned longitudinally in the sagittal plane at 6 μm thickness using a rotary microtome (Leica RM2255; Germany).

To measure growth plate thickness, five evenly spaced lines were averaged for two slides per mouse, 6 mice per genotype on sections stained with Safranin O/Fast Green/Alcian Blue (OsteomeasureXP v3.2.1.7; Osteometrics).

To quantify osteoclast number, sections of the proximal tibiae were stained for TRAP. Sections were deparaffinized and rehydrated, and then placed in TRAP buffer for 10 minutes (3.28 g Na-acetate, 46.01 g Na-tartrate in 1 L distilled water; Sigma-Aldrich). Sections were then incubated at 37°C in TRAP staining solution for 100 minutes (40 mg Napthol AS-MIX, 4 mL N-N-dimethylformamide, 240 mg Fast Red Violett LB Salt, 2 mL Triton X-100; Sigma-Aldrich, in 200 mL TRAP buffer). After counterstaining with hematoxylin, sections were dehydrated and coverslipped. Beginning distal to the primary spongiosa, the number of positively-stained osteoclasts in the cancellous tissue normalized to bone surface was counted for two slides per mouse, 6 mice per genotype.

For procollagen I and ERα immunostaining, longitudinal sections of the proximal tibiae were deparaffinized and rehydrated. Antigen retrieval was achieved using 0.1 M hot citrate buffer (20 minutes procollagen I, 10 minutes ERα). Endogenous peroxidase blocking was performed with 2% hydrogen peroxide (5 minutes), 2.5% periodic acid (5 minutes), and 0.02% sodium borohydride (5 minutes). Protein blocking was done using serum-free protein block for 20 minutes for procollagen I (Dako) and using goat normal serum for 4 hours for ERα (Vectastain ABC kit). Sections were incubated in either anti-procollagen I primary antibody (undiluted, SP1.D8; Developmental Studies Hybridoma Bank, Iowa City, IA, USA) or anti-ERα primary antibody (1:100; Abcam, Cambridge, MA, USA; 75635) overnight. Secondary antibody was delivered for 1 hour (anti-mouse immunoglobulin G [IgG] for procollagen I and anti-rabbit IgG for ERα; Vectastain ABC kits), and staining was visualized using diaminobenzidine. Sections were dehydrated and coverslipped. For osteoblast activity, the number of positively-stained osteoblasts for procollagen I was counted and normalized to bone surface for two slides per mouse, 6 mice per genotype in the cancellous tissue beginning distal to the primary spongiosa.

Mechanical testing

Prior to testing all bones were thawed to room temperature and kept moist in PBS. Femur length, and vertebral height, length, and width were measured using calipers. Right femora were loaded to failure in three-point bending in the anterior-posterior direction with a span length of 6 mm at a rate of 0.1 mm/s (858 Mini Bionix; MTS, Eden Prairie, MN, USA). L5 vertebrae were loaded in compression at a rate of 0.05 mm/s to failure. For femora, bending strength and stiffness were calculated from load and displacement data. For vertebrae, compressive strength and stiffness were calculated.[27]

Statistics

Differences between pOC-ERαKO and LC mice for mass, serum (except for TRACP5b), and histomorphometry were determined using Student's *t* tests in each age group. For μCT, mechanical testing, TRACP5b serum levels, and histology (procollagen I, TRAP, growth plate thickness), a two-factor ANOVA (age, genotype) with interaction was used with Tukey's honestly significant difference (HSD) post hoc (JMP Pro 10). Significance was set at $p < 0.05$.

Results

Generation and characterization of pOC-ERαKO mice

To study the effects of ERα absence in osteoblasts on bone strength, we crossed mice expressing the floxed ERα gene with animals transgenic for *Cre* driven by the human osteocalcin promoter. Mice were viable and born at the expected Mendelian ratio. The absence of ERα in osteoblasts in pOC-ERαKO mice was confirmed by PCR of genomic DNA of femoral shafts and ERα immunohistochemistry (IHC) in the proximal tibia (Supplementary Fig. 1). As others have reported, we found *Cre* expression in hypertrophic chondrocytes in addition to osteoblasts and osteocytes when *OC-Cre* mice were crossed with *ROSA26-Cre* reporter mice and longitudinal tibial sections were stained with X-Gal to detect β-galactosidase activity (data not shown).[28] However, we found no subsequent growth plate effects in the pOC-ERαKO mice. Specifically, the growth plates in the pOC-ERαKO mice had normal cell alignment and organization, and did not differ in thickness compared to LC mice at 12 or 18 weeks of age (Fig. 1, Table 1). In addition, femoral and tibial lengths were not different between pOC-ERαKO and LC mice in either age group, indicating normal endochondral ossification and longitudinal bone growth (Supplementary Table 1).

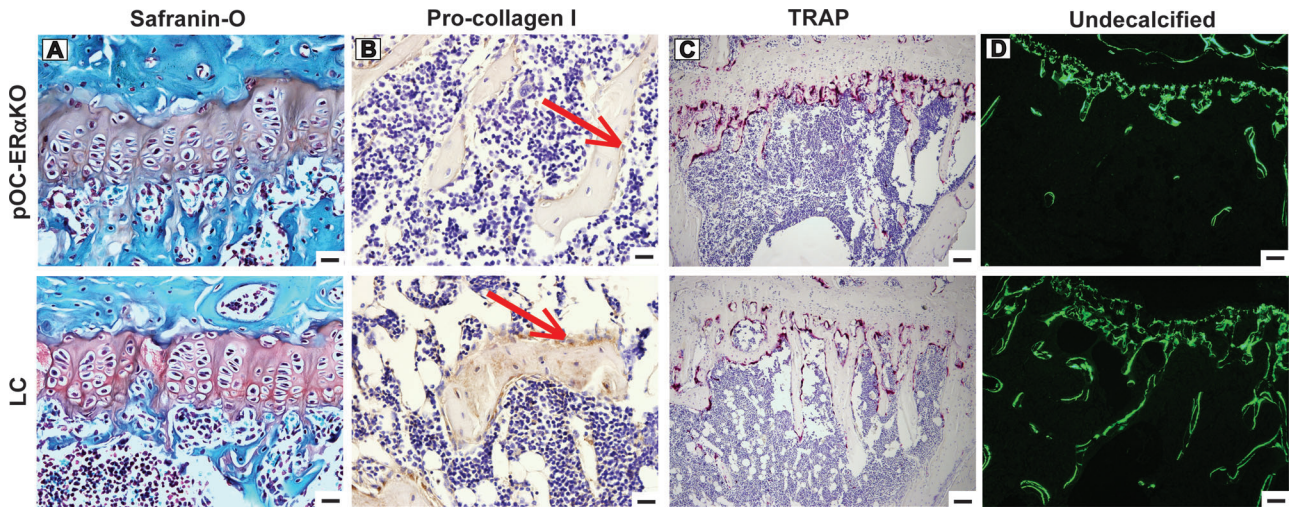

Fig. 1. Representative IHC, histology, and dynamic histomorphometry images for sagittal sections of the proximal tibiae of pOC-ERαKO and LC female mice. (*A*) Tibial growth plate thickness did not differ between pOC-ERαKO and LC based upon measures from growth plates stained with Safranin-O. (*B*) In the cancellous bone of the proximal tibia, fewer osteoblasts per bone surface were positive for procollagen I activity (red arrow) in pOC-ERαKO compared to LC. (*C*) Osteoclast number normalized to bone surface was similar between pOC-ERαKO and LC mice at both age groups as indicated by TRAP staining in cancellous bone in the proximal tibia. (*D*) Reduced cancellous bone volume fraction is apparent in undecalcified sections of the proximal tibiae in pOC-ERαKO mice compared to LC. Dynamic histomorphometry measurements from double calcein labeling were not significantly different between genotypes. Scale bar = 20 μm for *A*, *B*; 80 μm for *C*, *D*. *A–C* are at 12 weeks and *D* is at 18 weeks.

In contrast to the global ERαKO mice, systemic effects were not present in our osteoblast-specific ERαKO mice. No differences in body, ovarian, or uterine mass were measured between female pOC-ERαKO and LC mice (Supplementary Fig. 2). Altered serum levels of E2, T, IGF-1, and OC found in the global ERαKO mouse that may have produced secondary skeletal effects were eliminated in this tissue-specific knockout model; these parameters were all similar between pOC-ERαKO female mice and LC (Fig. 2).

Bone mass and architecture

Previously, bone mass was altered in both global and bone-specific ERαKO mice. In our osteoblast-specific ERαKO mouse, cancellous bone mass was severely reduced at the three sites examined compared to LC mice at 12 weeks of age (Fig. 3, Table 2). Bone volume fraction (BV/TV) was significantly reduced in the proximal tibia (−35%), L5 vertebral body (−35%), and distal femur (−30%). The same decrease in all measured parameters continued in 18-week-old animals. Mean BV/TV remained significantly less in the proximal tibia (−7%), vertebra (−44%), and distal femur (−33%) of pOC-ERαKO mice at 18 weeks of age as well.

Changes in cancellous trabecular architecture correlated with decreased bone mass (Table 2). Reduced BV/TV in pOC-ERαKO mice was due primarily to increased trabecular separation (Tb.Sp), which was markedly increased in all three cancellous sites at both ages. The proximal tibia had the greatest increase in Tb.Sp, which was increased 45% at 12 weeks and 60% at 18 weeks in pOC-ERαKO mice. In the distal femur, Tb.Sp was increased in pOC-ERαKO mice compared to LC in both 12-week-old and 18-week-old animals (+40% and +76%, respectively), and in the vertebra (+14% and +25% for 12 weeks and 18 weeks of age, respectively). Regardless of bone site or genotype, Tb.Sp increased with age in all animals. Trabecular thickness (Tb.Th) was decreased in pOC-ERαKO mice compared to LC in both age groups only in the vertebra (−14% and −21% at 12 weeks and 18 weeks, respectively), contributing to the overall reduced vertebral BV/TV. Tb.Th, like Tb.Sp, increased significantly with age in the tibiae and vertebra, but not in the femur.

Table 1. IHC and Histology Quantification for the Proximal Tibia of pOC-ERαKO and LC mice

	12 weeks old		18 weeks old	
	LC	pOC-ERαKO	LC	pOC-ERαKO
GP.Th (mm)	0.117 ± 0.0051	0.114 ± 0.0038	0.106 ± 0.014	0.109 ± 0.024
N.Ob/BS (mm^{-1})	3.44 ± 1.8	2.00 ± 0.88[a]	2.07 ± 0.98	1.36 ± 1.1[a]
N.Ocl/BS (mm^{-1})	3.44 ± 0.21	3.47 ± 0.60	2.06 ± 0.65[b]	1.43 ± 0.46[b]

Values are mean ± SD.

IHC = immunohistochemistry; GP.Th = growth plate thickness; N.Ob = number of positively stained osteoblasts for pro-collagen I; BS = bone surface; N.Ocl = number of positively stained osteoclasts for TRAP; TRAP = tartrate-resistant acid phosphatase.

[a]pOC-ERαKO different from LC, $p < 0.05$ by two-factor ANOVA with interaction.

[b]18 weeks old different from 12 weeks old, $p < 0.05$ by two-factor ANOVA with interaction.

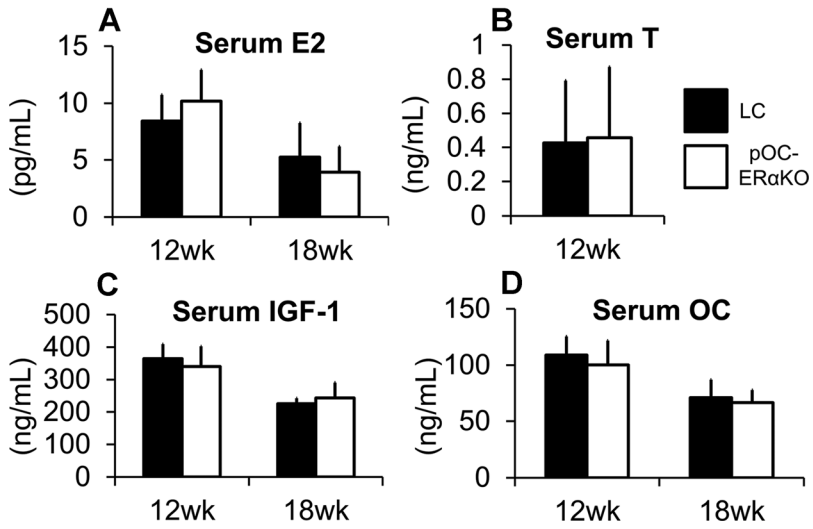

Fig. 2. Unlike global ERαKO mice, serum levels of estrogen (*A*), testosterone (*B*), IGF-1 (*C*), and osteocalcin (*D*) were unaltered in female pOC-ERαKO mice compared to controls at both 12 and 18 weeks of age ($n = 6$–10 per genotype per age). Data are shown as mean ± SD.

Cancellous tissue mineral density (cn.TMD) was not affected by osteoblast-specific deletion of ERα (Table 2). However, cn.TMD decreased significantly with age at the proximal tibia (−3% LC, −5% pOC-ERαKO) but increased with age in the distal femur (+4% LC, +2% pOC-ERαKO).

The cancellous changes in the corticocancellous distal femur and vertebra of pOC-ERα mice were accompanied by analogous but smaller cortical changes (Fig. 3, Table 3). Cortical area (Ct.Ar) was reduced in the distal femur and L5 vertebra cortexes in pOC-ERαKO mice compared to LC at 12 weeks (−13% and −4%, respectively) and 18 weeks (−14% and −11%, respectively). This decrease in bone mass corresponded with lower overall cortical thickness (Ct.Th) at both sites at 12 weeks (−8% for femur, −10% for vertebra) and 18 weeks (−14% for both bones). In the distal femur only, maximum and minimum moments of inertia (I_{MAX}, I_{MIN}, respectively) were reduced at 12 weeks in pOC-ERαKO mice (−16% and −17%, respectively) and at 18 weeks (−11% and −12%, respectively). In both genotypes, femoral Ct.Ar was greater in mice 18 weeks old than 12 weeks old (+11% for LC, +10% for pOC-ERαKO) as were I_{MAX} and I_{MIN} (+16% for both in LC, +23% for both in pOC-ERαKO). Tissue mineral density in the cortical shell (ct.TMD) was reduced in pOC-ERαKO mice

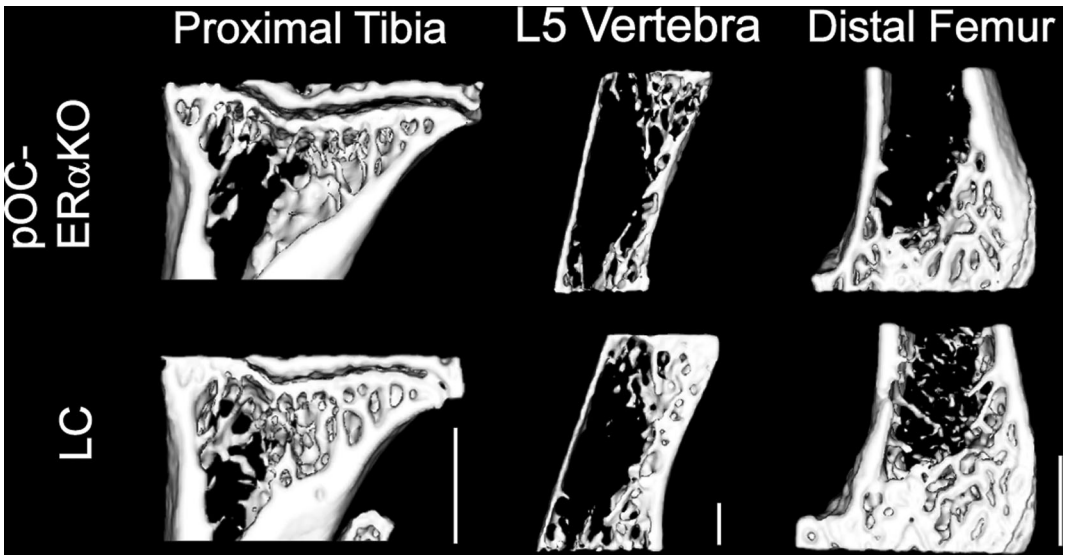

Fig. 3. Lack of ERα in osteoblasts significantly reduced cancellous and cortical bone mass in pOC-ERαKO female mice. Sagittal sections through the proximal tibiae, L5 vertebrae, and distal femora are shown from representative μCT scans of 12-week-old female pOC-ERαKO and LC mice. Bone volume fraction was reduced 35% in the proximal tibia, 35% in the L5 vertebra, and 30% in the distal femur. Cortical area was reduced 4% in the L5 vertebra and 13% in the distal femur. Scale bar = 0.5 mm for tibia and vertebra and 1.0 mm for femur.

Table 2. Cancellous Parameters Measured by μCT for the Proximal Tibia, L5 Vertebral Body, and Distal Femur of 12-Week-Old and 18-Week-Old Female pOC-ERαKO and LC Mice

	Proximal tibia		L5 vertebra		Distal femur	
	LC	pOC-ERαKO	LC	pOC-ERαKO	LC	pOC-ERαKO
12-week-old						
BV/TV	0.0964 ± 0.023	0.0630 ± 0.016^{a}	0.246 ± 0.054	0.160 ± 0.041^{a}	0.118 ± 0.028	0.0819 ± 0.019^{a}
Tb.Th (μm)	51.4 ± 4.2	50.0 ± 3.2	55.4 ± 5.7	47.6 ± 4.4^{a}	55.9 ± 3.3	52.6 ± 3.2
Tb.Sp (μm)	333 ± 44	484 ± 47^{a}	236 ± 33	269 ± 31^{a}	264 ± 31	368 ± 79^{a}
cn.TMD (mg HA/cm^3)	771 ± 16	775 ± 18	657 ± 43	667 ± 41	706 ± 21	709 ± 20
18-week-old						
BV/TV	0.134 ± 0.020^{b}	$0.125 \pm 0.035^{a,b}$	0.272 ± 0.047	0.154 ± 0.025^{a}	0.0968 ± 0.031^{b}	$0.0648 \pm 0.022^{a,b}$
Tb.Th (μm)	64.2 ± 6.3^{b}	68.5 ± 5.3^{b}	63.9 ± 13^{b}	$50.6 \pm 2.7^{a,b}$	53.7 ± 7.3	53.2 ± 5.3
Tb.Sp (μm)	352 ± 55^{b}	$563 \pm 122^{a,b}$	249 ± 28^{b}	$311 \pm 37^{a,b}$	308 ± 32^{b}	$542 \pm 122^{a,b}$
cn.TMD (mg HA/cm^3)	750 ± 16^{b}	737 ± 14^{b}	674 ± 27	660 ± 13	732 ± 14^{b}	772 ± 18^{b}

Values are mean ± SD.

μCT = microcomputed tomography; BV/TV = bone volume fraction; Tb.Th = trabecular thickness; Tb.Sp = trabecular separation; cn.TMD = cancellous tissue mineral density; HA = hydroxyapatite.

[a]pOC-ERαKO different from LC, $p < 0.05$ by two-factor ANOVA with interaction.

[b]18-week-old different from 12-week-old, $p < 0.05$ by two-factor ANOVA with interaction.

compared to LC at both ages in the distal femur (−2% at 12 weeks, −3% at 18 weeks), but not in the L5 vertebra. However, ct.TMD increased with age in the L5 vertebra, by 2% in LC and 3% in pOC-ERαKO mice. In the corticocancellous regions of the distal femur and L5 vertebra, decreased bone mass in pOC-ERαKO mice was present in both the cortical shell and the cancellous cortex.

Cortical bone mass was also reduced compared to LC in the tibial diaphysis, but less so than in the cancellous envelope of the metaphysis (Fig. 4). At the tibial midshaft, Ct.Ar was decreased in both 12-week-old and 18-week-old female pOC-ERαKO mice compared to LC (−8% and −7%, respectively) (Table 3). At both ages, this decrease in bone mass was due to decreased Ct.Th (−7% at both ages) and lower ct.TMD (−2% at 12 weeks, −1% at 18 weeks). In older animas, Ct.Th and ct.TMD were significantly greater than younger animals for both genotypes. I_{MAX} at the tibial midshaft was not affected by osteoblast-specific ERα deletion, but I_{MIN} was significantly reduced in pOC-ERαKO mice at both ages (−19% at 12 weeks and −14% at 18 weeks). Marrow area in the tibial midshaft was also unchanged by ERα deletion in osteoblasts; thus, the smaller cortex reflected a lack of periosteal expansion along the minimum axis.

Table 3. Cortical Parameters Measured by μCT for the Tibial Midshaft, L5 Vertebra, and Distal Femur of 12-Week-Old and 18-Week-Old Female pOC-ERαKO and LC Mice

	Tibial midshaft		L5 vertebra		Distal femur	
	LC	pOC-ERαKO	LC	pOC-ERαKO	LC	pOC-ERαKO
12-week-old						
Ct.Ar (mm^2)	0.654 ± 0.057	0.601 ± 0.071^{a}	0.477 ± 0.065	0.460 ± 0.058^{a}	1.09 ± 0.12	0.948 ± 0.10^{a}
T.Ar (mm^2)	0.928 ± 0.083	0.871 ± 0.10	–	–	–	–
Ma.Ar (mm^2)	0.275 ± 0.041	0.270 ± 0.054	–	–	–	–
Ct.Th (mm)	0.240 ± 0.014	0.223 ± 0.0097^{a}	0.0909 ± 0.010	0.0817 ± 0.0056^{a}	0.168 ± 0.014	0.154 ± 0.023^{a}
I_{MAX} (mm^4)	0.0791 ± 0.015	0.0747 ± 0.018	0.198 ± 0.037	0.213 ± 0.047	0.554 ± 0.10	0.465 ± 0.099^{a}
I_{MIN} (mm^4)	0.0514 ± 0.0094	0.0415 ± 0.010^{a}	0.0614 ± 0.018	0.0575 ± 0.014	0.277 ± 0.069	0.231 ± 0.049^{a}
ct.TMD (mg HA/cm^3)	1020 ± 17	1000 ± 15^{a}	713 ± 27	707 ± 18	882 ± 29	868 ± 37^{a}
18-week-old						
Ct.Ar (mm^2)	0.677 ± 0.059	0.628 ± 0.063^{a}	0.501 ± 0.052	0.445 ± 0.039^{a}	1.21 ± 0.083^{b}	$1.04 \pm 0.10^{a,b}$
T.Ar (mm^2)	0.923 ± 0.098	0.887 ± 0.10	–	–	–	–
Ma.Ar (mm^2)	0.246 ± 0.055	0.259 ± 0.061	–	–	–	–
Ct.Th (mm)	0.256 ± 0.016^{b}	$0.237 \pm 0.017^{a,b}$	0.0948 ± 0.0051	0.0816 ± 0.0048^{a}	0.175 ± 0.013	0.150 ± 0.0094^{a}
I_{MAX} (mm^4)	0.0796 ± 0.020	0.0764 ± 0.016	0.219 ± 0.052	0.209 ± 0.033	0.643 ± 0.076^{b}	$0.573 \pm 0.097^{a,b}$
I_{MIN} (mm^4)	0.0511 ± 0.0092	0.0439 ± 0.011^{a}	0.0621 ± 0.010	0.0628 ± 0.011	0.322 ± 0.049^{b}	$0.285 \pm 0.045^{a,b}$
ct.TMD (mg HA/cm^3)	1040 ± 12^{b}	$1020 \pm 14^{a,b}$	724 ± 32^{b}	725 ± 21^{b}	899 ± 18	875 ± 14^{a}

Values are mean ± SD.

μCT = microcomputed tomography; Ct.Ar = cortical area; T.Ar = total area; Ma.Ar = marrow area; Ct.Th = cortical thickness; I_{MAX}/I_{MIN} = maximum/minimum moment of inertia; ct.TMD = cortical tissue mineral density; HA = hydroxyapatite.

[a]pOC-ERαKO different from LC, $p < 0.05$ by two-factor ANOVA with interaction.

[b]18-week-old different from 12-week-old, $p < 0.05$ by two-factor ANOVA with interaction.

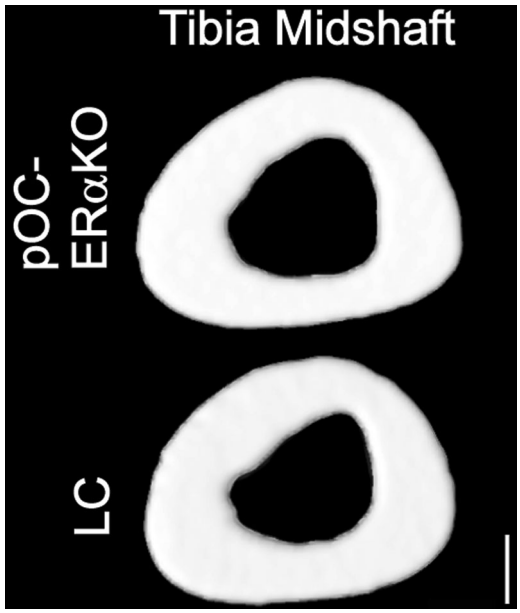

Fig. 4. Deletion of ERα from osteoblasts reduced cortical bone mass. Transverse sections at the tibial midshaft from μCT scans of 12-week-old female pOC-ERαKO (top) and LC mice (bottom) are shown. Cortical area was 8% less in 12-week-old pOC-ERαKO mice compared to LC. Scale bar = 0.25 mm.

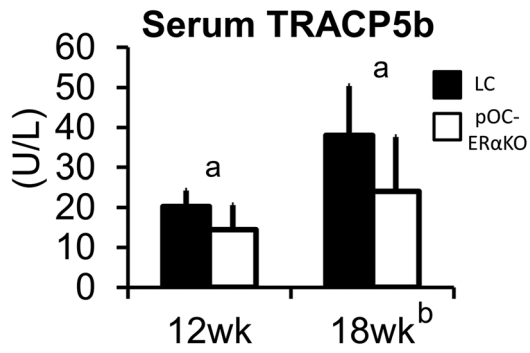

Fig. 5. pOC-ERαKO mice had significantly lower TRACP5b levels at both 12 and 18 weeks of age, indicating reduced osteoclast number resulting from lower bone mass. Data are represented as mean ± SD. [a]pOC-ERαKO different from LC, [b]18 weeks different from 12 weeks, $p < 0.05$ by two-factor ANOVA with interaction.

Bone cell activity

Decreased BV/TV in the cancellous tissue of the proximal tibiae of pOC-ERαKO mice reflected changes in osteoblast activity (Fig. 1). When normalized to bone surface, the number of procollagen I–positive osteoblasts was decreased in pOC-ERαKO females compared to LC at 12 weeks (−42%) and 18 weeks (−34%) (Table 1). Systemically, serum TRACP5b levels were reduced in pOC-ERαKO mice at both 12 weeks (−29%) and 18 weeks (−37%), reflecting the decreased cancellous bone mass (Fig. 5). However, local osteoclast number indicated by TRAP staining was not different between genotypes at either age when normalized to bone surface in the proximal tibia (Fig. 1, Table 1).

Decreased bone mass was evident in undecalcified longitudinal sections of the proximal tibia of pOC-ERαKO animals (Fig. 1), but dynamic histomorphometric measurements were not statistically different between genotypes for either cancellous bone in the proximal tibia or at endosteal or periosteal surfaces at the tibial midshaft.

Whole bone strength

The decreases in cortical and cancellous bone mass and compromised architecture resulting from deletion of ERα in osteoblasts corresponded to compromised whole bone strength. In both age groups, vertebral and femoral strength were reduced in pOC-ERαKO mice compared to LC, as determined through mechanical testing to failure (Fig. 6). Femoral bending strength was reduced 11% at 12 weeks and 10% at 18 weeks, whereas vertebral strength was reduced 25% at both ages in pOC-ERαKO mice. Bone strength increased significantly with age (+27% femur, +17% vertebra for pOC-ERαKO; +26% femur, +18% vertebra for LC). Interestingly, vertebral compressive strength correlated linearly with BV/TV for LC but not pOC-ERαKO mice through regression analysis (Supplementary Fig. 3). BV/TV accounted for 43% of the variation in vertebral compressive strength for LC mice ($p = 0.0006$) but BV/TV had no predictive value for vertebral strength in pOC-ERαKO mice. Although femoral bending stiffness was decreased in pOC-ERαKO mice compared to LC at both 12 weeks (−13%) and 18 weeks (−15%), vertebral compressive stiffness was not significantly different between genotypes. Femoral and vertebral stiffness also increased significantly with age (+40% femur, +43% vertebra for pOC-ERαKO; +42% femur, +34% vertebra for LC).

Discussion

We successfully deleted ERα from osteoblasts and osteocytes in female mice by mating *ERα*$^{fl/fl}$ and *OC-Cre* mice without producing systemic hormone effects. Serum E2, T, IGF-1, and OC were unchanged in pOC-ERαKO mice, as were ovarian and uterine masses, confirming the lack of systemic effects that may independently alter bone phenotype. During growth, the pOC-ERαKO and LC mice did not differ in body mass, and long-bone lengths were similar between genotypes at both 12 and 18 weeks of age. In contrast, the pOC-ERαKO mice had decreased cancellous and cortical bone mass compared to littermate controls, which negatively impacted whole-bone strength and stiffness, indicating that ERα in osteoblasts is a critical component of successful accrual of bone mass and strength in female mice.

The role of ERα in bone was studied initially using global ERαKO mice, which have a drastically different skeletal phenotype opposite that seen in our pOC-ERαKO and other osteoblast-specific ERαKO mouse models.[11–13] Whereas our pOC-ERαKO female mice had decreased cancellous and cortical bone mass, the global ERαKO female mice had increased bone mass and bone mineral density.[16,17] However, systemic effects indicate that other tissues were affected by global ERα deletion. Female mice had increased serum estrogen levels leading to increased uterine mass and decreased serum IGF-1 levels resulting in shorter bones.[12,15,17,18] Because estrogen and IGF-1 have major indirect actions on bone,[29,30] the skeletal phenotype seen in the global ERαKO mice is influenced by these secondary

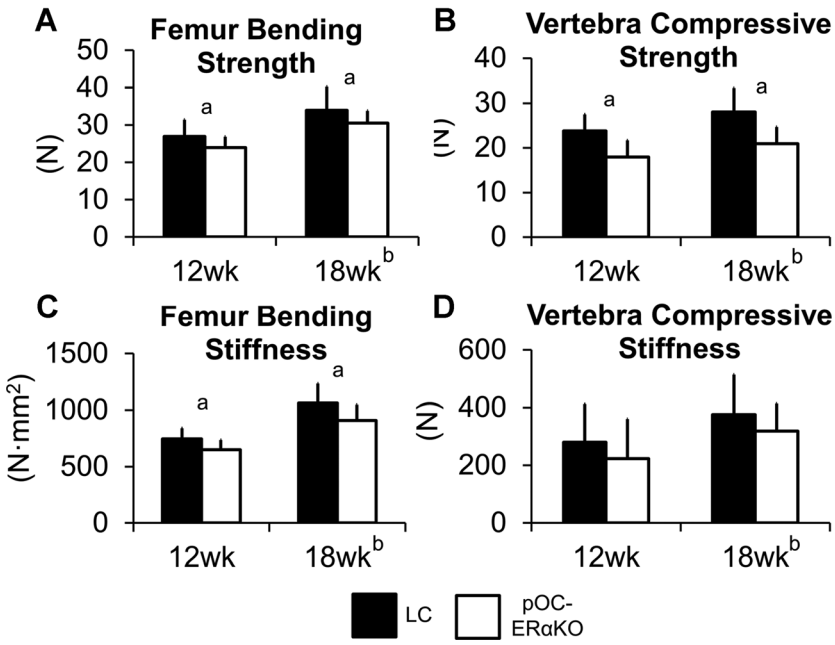

Fig. 6. Whole-bone strength and stiffness were compromised in pOC-ERαKO female mice. (*A*) In three-point bending to failure, pOC-ERαKO female mice had decreased femoral bending strength at both 12 weeks (−11%) and 18 weeks (−10%) of age. (*B*) L5 vertebrae of pOC-ERαKO female mice were 25% weaker at both 12 and 18 weeks of age in compression testing to failure. (*C*) Femur bending stiffness was reduced 13% and 15% in 12-week-old and 18-week-old pOC-ERαKO mice, respectively, compared to LC. (*D*) Vertebral compressive stiffness was not different between genotypes. $n = 10$–17 per genotype and age. Data are represented as mean ± SD. [a]pOC-ERαKO different from LC, [b]18 weeks different from 12 weeks, $p < 0.05$ by two-factor ANOVA with interaction.

effects and those arising from the direct role of ERα in bone. These conflicting results led researchers to create conditional knockouts, such as our pOC-ERαKO mouse.

Estrogen acts in bone-residing cells primarily through ERα to alter gene transcription, but also exhibits non-genomic effects[31,32] and so is likely to have distinct effects on different lineages as they mature and differentiate, as has been shown though osteoblast lineage deletions of receptor activator of NF-κB ligand (RANKL).[28] Recently, two other conditional ERαKO mouse models focusing on osteoblasts were generated, with results that are similar to ours or in significant conflict with ours. Määttä and colleagues[20] also used the *OC-Cre* promoter transgenic mouse to create animals with an osteoblast-specific deletion of ERα ($ER\alpha^{\Delta OB/\Delta OB}$).[20] Bone phenotype was analyzed in both males and females at 3.5, 6, and 12 months of age. As in our 12-week-old and 18-week-old pOC-ERαKO mice, BV/TV in the proximal tibia and cortical bone volume at the tibial diaphysis were reduced in female $ER\alpha^{\Delta OB/\Delta OB}$ mice at 3.5 months. However, this phenotype disappeared with age. At 6 months, bone mass was still decreased in the proximal tibia, but Tb.Sp was no longer different between genotypes; whereas by 12 months of age, no tibial cancellous phenotype difference was seen by μCT analysis. We cannot confirm their results for older mice, as our study only included growing (12 weeks old) and skeletally mature (18 weeks old) animals.

In contrast to the work of Määttä and colleagues[20] and our study, Almeida and colleagues[19] found no cortical or cancellous bone phenotype in a female osteoblast-specific ERαKO mouse ($ER\alpha^{f/f}$*;Col1a1-Cre*), using the *Col1a1-Cre* promoter, which is expressed in mature osteoblasts and osteocytes. Femoral cancellous bone mass and cortical thickness were unaltered in 12-week-old and 26-week-old female mice, and spine and femoral bone mineral density (BMD) were unchanged in female mice from 4 to 12 weeks of age. However, when the same authors deleted ERα in osteoblast progenitor cells using either *Osx-Cre* or *Prx-Cre* mice, BMD of the femur and cortical thickness in the femur mid-diaphysis were decreased in female mice, but cancellous bone mass remained unchanged at the proximal femur. These findings indicate that ERα is not required in either osteoblasts or their progenitors for cancellous bone mass accrual in females; in contrast, cortical bone was affected by absence of ERα in osteoblast progenitors but not mature osteoblasts. Much of the discrepancy in the results found in $ER\alpha^{f/f}$*;Col1a1-Cre* model versus the $ER\alpha^{\Delta OB/\Delta OB}$ model and our pOC-ERαKO model can be attributed to the use of different *Cre* models and timing of their cellular effects. The *OC-Cre* targets osteoblasts during the mineralization phase, whereas the *Col1a1-Cre* targets osteoblasts earlier, during the matrix maturation phase.[33] Interestingly, when ERα was ablated only in mature osteocytes using the 10-kb *DMP1-Cre* mouse, cancellous and cortical bone were both unaffected in female mice, suggesting that, when combined with our study's results, ERα may play a stronger role in osteoblasts than in osteocytes.[21]

The *OC-Cre* mouse is an established model used to ablate genes in mature osteoblasts and osteocytes.[26] Crossing these mice with *ROSA26-Cre* reporter mice has shown that *Cre* expression is limited to osteoblasts and osteocytes, but expression in hypertrophic chondrocytes has been reported.[28,34] Because hypertrophic chondrocytes differentiate into osteoblasts during endochondral ossification, the possible effects of ERα in growth plate cartilage cannot be ignored when examining the bone phenotypes of pOC-ERαKO mice. In a cartilage-specific

ERαKO female mouse, the skeleton developed normally during growth, but continued to grow beyond 4 months of age, resulting in increased femur length compared to controls.[35] Femoral growth plate height, however, was not different between cartilage-specific ERαKO mice and controls, which is consistent with our results, in which tibial growth plate height and long bone lengths were similar between pOC-ERαKO and LC. In contrast, female $ER\alpha^{\Delta OB/\Delta OB}$ at 3.5 months of age had increased tibial growth plate height compared to controls but no difference in bone length.[20] Although we cannot explain the growth plate discrepancy between similarly generated mice, we can infer that the skeletal phenotype seen in pOC-ERαKO is indeed bone-mediated as opposed to cartilage-mediated because bone lengths and growth plate structure were unaffected.

Although mouse models cannot directly translate to human clinical data, ERα clearly plays an important role in both the mouse and human skeletons. In human clinical data, a mutation in the ERα gene increased BMD and resulted in osteopenic bone.[9] Polymorphisms in ERα are correlated with bone mass in humans.[36] Our data show that when ERα is deleted from osteoblasts, bone mass and strength are compromised at cortical and corticocancellous sites in female mice, pointing to a crucial role of ERα in these cells. The receptor has been proposed to be involved in a number of bone signaling networks, including those activated by estrogen, IGF-1, wnt/β-catenin, and bone morphogenic protein 2 (BMP-2).[37–39] The majority of these studies examined the interaction between estrogen signaling and other signaling pathways using osteoblast cultures in vitro. Availability of osteoblast-specific ERαKO mice will facilitate future studies on osteoblastic ERα signaling in vivo. As we increase our understanding of estrogen signaling in bone, we may have the opportunity to develop new drugs for preventing and treating osteoporosis, especially in postmenopausal women, in whom estrogen signaling is most relevant.

Disclosures

All authors state that they have no conflicts of interest.

Acknowledgments

This work was supported by National Institutes of Health grants R01-AG028664 and P30-AR046121 (to MCHM), NSF GRF (to KMM and NHK), and F32-AR054676 (to RPM). We thank the following for technical assistance: Timothy Bruhn, BS; Stephen Doty, PhD; Stephen Hong, BS; Alison Hsia, BS; Grace Kim, PhD; Frank Ko, MS; Eric Lee, BS; and Kerry Schimenti, BS. We are grateful to Cornell CARE Staff for their assistance. We thank Thomas Clemens, PhD, for providing the *OC-Cre* mice.

Authors' roles: Study design: MCHM, KMM, RPM, FPR, NHK, JSC, and SAK. Study conduct: KMM and NHK. Data collection: KMM and NHK. Data analysis: KMM. Data interpretation: KMM, MCHM, and FPR. Drafting manuscript: KMM. Revising manuscript content: KMM, MCHM, FPR, NHK, and RPM. Approving final version of manuscript: all authors. KMM takes responsibility for the integrity of the data analysis.

References

1. Bone Health and Osteoporosis: A Report of the Surgeon General. Rockville, MD: U.S. Department of Health and Human Services, Office of the Surgeon General; 2004.
2. Burge R, Dawson-Hughes B, Solomon DH, Wong JB, King A, Tosteson A. Incidence and economic burden of osteoporosis-related fractures in the United States, 2005–2025. J Bone Miner Res. 2007;22(3): 465–75.
3. Manolagas SC, Bellido T, Jilka RL. Sex steroids, cytokines and the bone marrow: new concepts on the pathogenesis of osteoporosis. Ciba Found Symp. 1995;191:187–96.
4. Eastell R. Role of oestrogen in the regulation of bone turnover at the menarche. J Endocrinol. 2005;185(2):223–34.
5. Riggs BL. The mechanisms of estrogen regulation of bone resorption. J Clin Invest. 2000;106(10):1203–4.
6. Richelson LS, Wahner HW, Melton LJ 3rd, Riggs BL. Relative contributions of aging and estrogen deficiency to postmenopausal bone loss. N Engl J Med. 1984;311(20):1273–5.
7. Riggs BL. Endocrine causes of age-related bone loss and osteoporosis. Novartis Found Symp. 2002;242:247–59.
8. Johnell O, Kanis JA. An estimate of the worldwide prevalence and disability associated with osteoporotic fractures. Osteoporos Int. 2006;17(12):1726–33.
9. Smith EP, Boyd J, Frank GR, et al. Estrogen resistance caused by a mutation in the estrogen-receptor gene in a man. N Engl J Med. 1994;331(16):1056–61.
10. Khosla S, Amin S, Orwoll E. Osteoporosis in men. Endocr Rev. 2008;29(4):441–64.
11. Lubahn DB, Moyer JS, Golding TS, Couse JF, Korach KS, Smithies O. Alteration of reproductive function but not prenatal sexual development after insertional disruption of the mouse estrogen receptor gene. Proc Natl Acad Sci U S A. 1993;90(23):11162–6.
12. Couse JF, Curtis SW, Washburn TF, et al. Analysis of transcription and estrogen insensitivity in the female mouse after targeted disruption of the estrogen receptor gene. Mol Endocrinol. 1995; 9(11):1441–54.
13. Dupont S, Krust A, Gansmuller A, Dierich A, Chambon P, Mark M. Effect of single and compound knockouts of estrogen receptors alpha (ERalpha) and beta (ERbeta) on mouse reproductive phenotypes. Development. 2000;127(19):4277–91.
14. Lee KC, Jessop H, Suswillo R, Zaman G, Lanyon LE. The adaptive response of bone to mechanical loading in female transgenic mice is deficient in the absence of oestrogen receptor-alpha and -beta. J Endocrinol. 2004;182(2):193–201.
15. Vidal O, Lindberg M, Sävendahl L, et al. Disproportional body growth in female estrogen receptor-alpha-inactivated mice. Biochem Biophys Res Commun. 1999;265(2):569–71.
16. Sims NA, Dupont S, Krust A, et al. Deletion of estrogen receptors reveals a regulatory role for estrogen receptors-beta in bone remodeling in females but not in males. Bone. 2002;30(1):18–25.
17. Lindberg MK, Alatalo SL, Halleen JM, Mohan S, Gustafsson JA, Ohlsson C. Estrogen receptor specificity in the regulation of the skeleton in female mice. J Endocrinol. 2001;171(2):229–36.
18. Parikka V, Peng Z, Hentunen T, et al. Estrogen responsiveness of bone formation in vitro and altered bone phenotype in aged estrogen receptor-alpha-deficient male and female mice. Eur J Endocrinol. 2005;152(2):301–14.
19. Almeida M, Iyer S, Martin-Millan M, et al. Estrogen receptor-alpha signaling in osteoblast progenitors stimulates cortical bone accrual. J Clin Invest. 2013;123(1):394–404.
20. Määttä JA, Büki KG, Gu G, et al. Inactivation of estrogen receptor alpha in bone-forming cells induces bone loss in female mice. FASEB J. 2012;27(2):478–88.
21. Windahl SH, Börjesson AE, Farman HH, et al. Estrogen receptor-alpha in osteocytes is important for trabecular bone formation in male mice. Proc Natl Acad Sci U S.A. 2013;110(6):2294–9.
22. Nakamura T, Imai Y, Matsumoto T, et al. Estrogen prevents bone loss via estrogen receptor alpha and induction of Fas ligand in osteoclasts. Cell. 2007;130(5):811–23.
23. Martin-Millan M, Almeida M, Ambrogini E, et al. The estrogen receptor-alpha in osteoclasts mediates the protective effects of estrogens on cancellous but not cortical bone. Mol Endocrinol. 2010;24(2):323–34.

24. van der Meulen MC, Jepsen KJ, Mikic B. Understanding bone strength: size isn't everything. Bone. 2001;29(2):101–4.
25. Clemens TL, Tang H, Maeda S, et al. Analysis of osteocalcin expression in transgenic mice reveals a species difference in vitamin D regulation of mouse and human osteocalcin genes. J Bone Miner Res. 1997;12(10):1570–6.
26. Zhang M, Xuan S, Bouxsein ML, et al. Osteoblast-specific knockout of the insulin-like growth factor (IGF) receptor gene reveals an essential role of IGF signaling in bone matrix mineralization. J Biol Chem. 2002;277(46):44005–12.
27. Turner CH, Burr DB. Basic biomechanical measurements of bone: a tutorial. Bone. 1993;14(4):595–608.
28. Xiong J, Onal M, Jilka RL, Weinstein RS, Manolagas SC, O'Brien CA. Matrix-embedded cells control osteoclast formation. Nat Med. 2011;17(10):1235–41.
29. Khosla S, Oursler MJ, Monroe DG. Estrogen and the skeleton. Trends Endocrinol Metab. 2012;23(11):576–81.
30. Canalis E. Growth factor control of bone mass. J Cell Biochem. 2009;108(4):769–77.
31. Almeida M, Han L, O'Brien CA, Kousteni S, Manolagas SC. Classical genotropic versus kinase-initiated regulation of gene transcription by the estrogen receptor alpha. Endocrinology. 2006; 147(4):1986–96.
32. Kousteni S, Bellido T, Plotkin LI, et al. Nongenotropic, sex-nonspecific signaling through the estrogen or androgen receptors: dissociation from transcriptional activity. Cell. 2001;104(5):719–30.
33. Lian JB, Stein JL, Stein GS, et al. Contributions of nuclear architecture and chromatin to vitamin D-dependent transcriptional control of the rat osteocalcin gene. Steroids. 2001;66(3–5):159–70.
34. Zhong Z, Zylstra-Diegel CR, Schumacher CA, et al. Wntless functions in mature osteoblasts to regulate bone mass. Proc Natl Acad Sci U S.A. 2012;109(33):E2197–04.
35. Börjesson AE, Lagerquist MK, Liu C, et al. The role of estrogen receptor alpha in growth plate cartilage for longitudinal bone growth. J Bone Miner Res. 2010;25(12):2690–700.
36. Wang KJ, Shi DQ, Sun LS, et al. Association of estrogen receptor alpha gene polymorphisms with bone mineral density: a meta-analysis. Chin Med J (Engl). 2012;125(14):2589–97.
37. Lau KH, Kapur S, Kesavan C, Baylink DJ. Up-regulation of the Wnt, estrogen receptor, insulin-like growth factor-I, and bone morphogenetic protein pathways in C57BL/6J osteoblasts as opposed to C3H/HeJ osteoblasts in part contributes to the differential anabolic response to fluid shear. J Biol Chem. 2006;281(14): 9576–88.
38. Price JS, Sugiyama T, Galea GL, Meakin LB, Sunters A, Lanyon LE. Role of endocrine and paracrine factors in the adaptation of bone to mechanical loading. Curr Osteoporos Rep. 2011;9(2):76–82.
39. Sunters A, Armstrong VJ, Zaman G, et al. Mechano-transduction in osteoblastic cells involves strain-regulated estrogen receptor alpha-mediated control of insulin-like growth factor (IGF) I receptor sensitivity to Ambient IGF, leading to phosphatidylinositol 3-kinase/AKT-dependent Wnt/LRP5 receptor-independent activation of beta-catenin signaling. J Biol Chem. 2010;285(12): 8743–58.

A

ERα IHC

LC

pOC-ERαKO

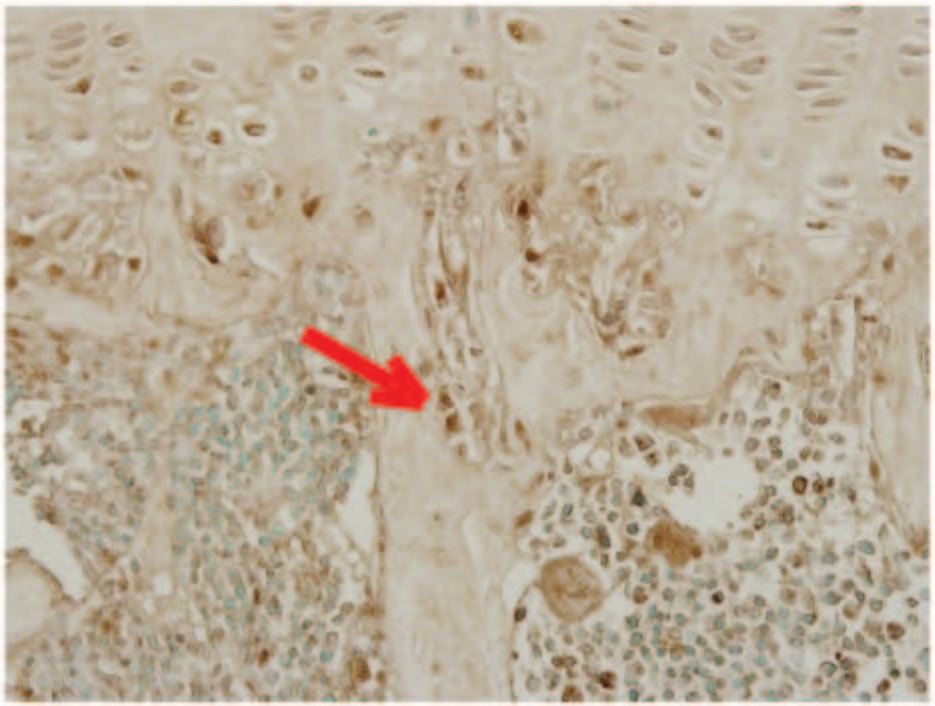

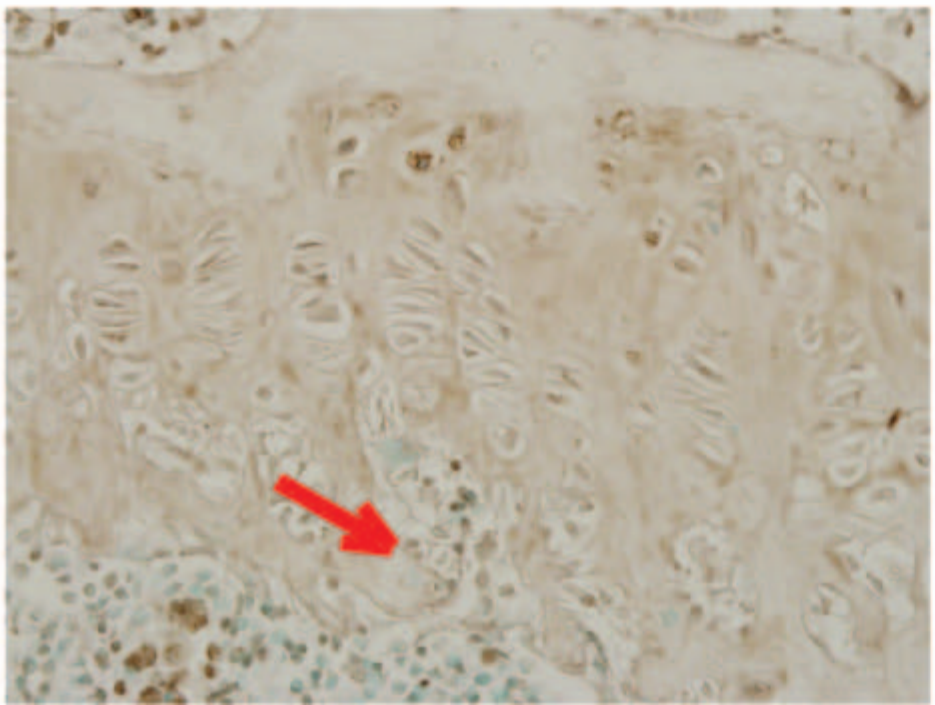

B

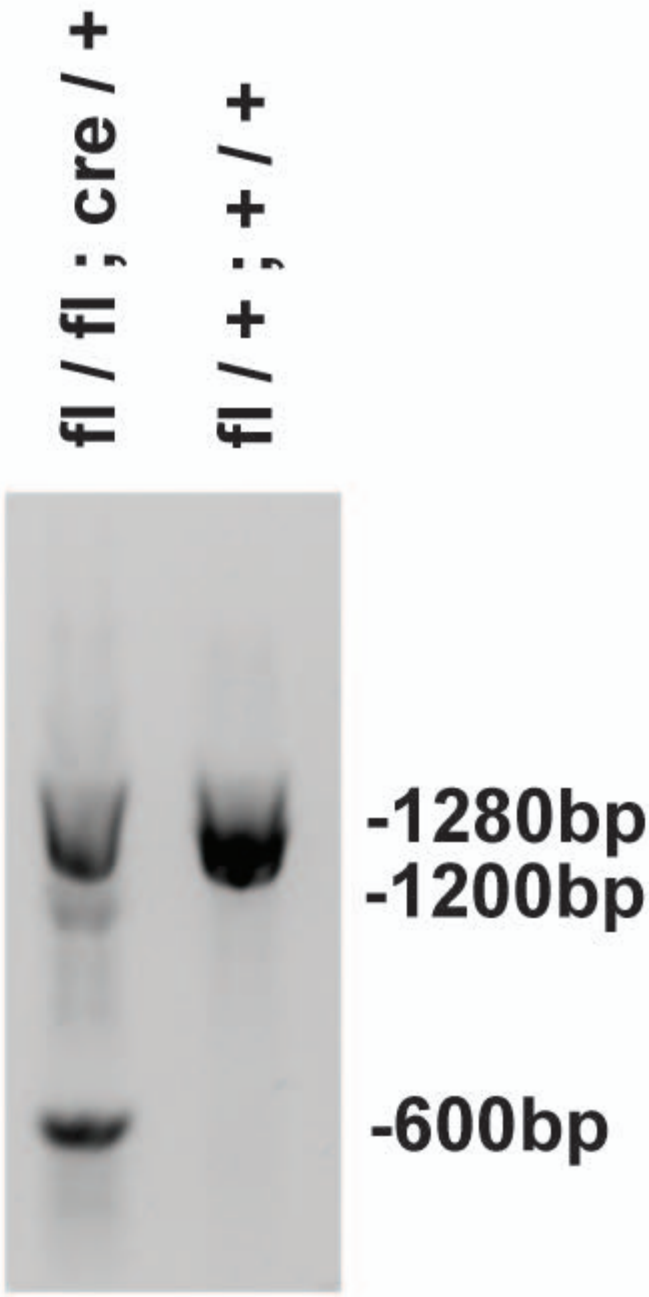

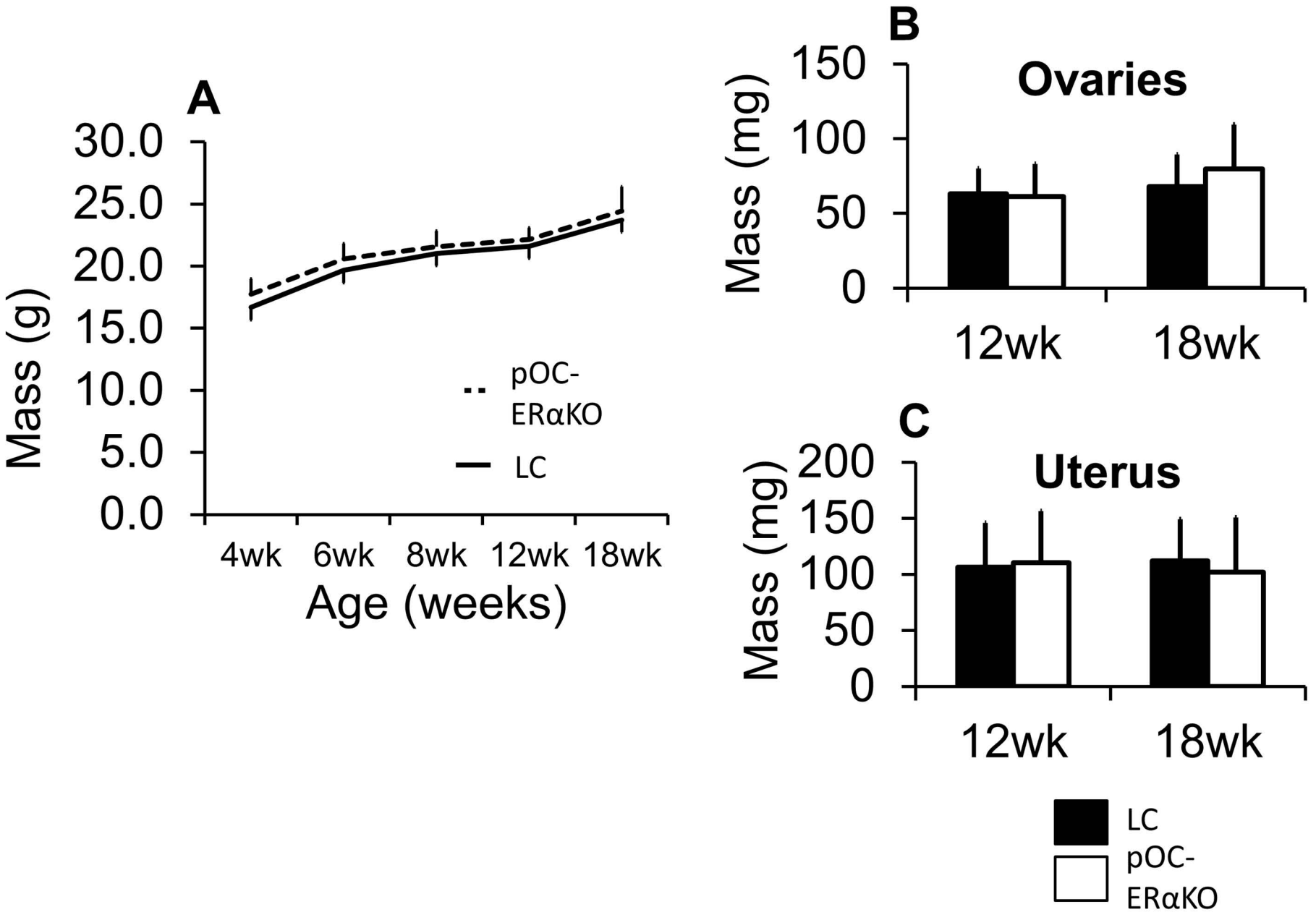
A
30.0
25.0
20.0
15.0
10.0
5.0
0.0
Mass (g)
4wk
6wk
8wk
12wk
18wk
Age (weeks)
pOC-
ERαKO
LC
B
Ovaries
150
100
50
0
Mass (mg)
12wk
18wk
C
Uterus
200
150
100
50
0
Mass (mg)
12wk
18wk
LC
pOC-
ERαKO

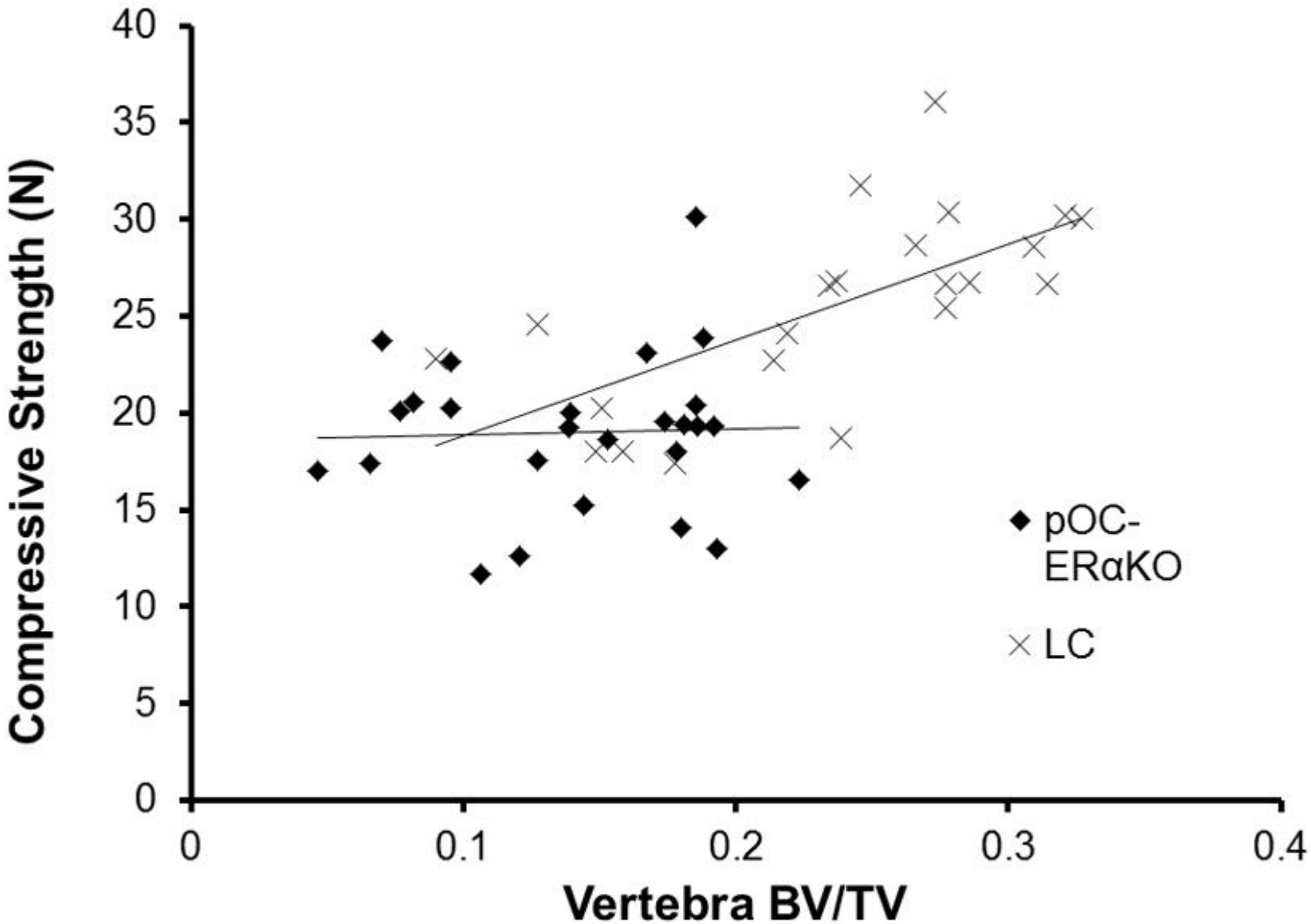
Compressive Strength (N)
40
35
30
25
20
15
10
5
0
0
0.1
0.2
0.3
0.4
Vertebra BV/TV
pOC-ERαKO
LC